Silicon
https://doi.org/10.1007/s12633-024-02895-z

RESEARCH

Distribution of Iron and Boron Between Silicon Metal Smelting Products in Industrial Saf using Borate Fluxes

Alexandr Alexandrovich Ilin[1] · Nikolay Nikolayevich Zobnin[1] · Irina Anatolyevna Pikalova[1] · Nina Vladimirovna Nemchinova[2]

Received: 13 November 2023 / Accepted: 1 February 2024

Abstract
The article identifies the key sources of iron and boron impurities entering silicon metal under industrial smelting conditions in Submerged arc furnace (SAF). Impurity rocks in the composition of quartz, the main raw material for the production of silicon metal, were studied using the X-ray fluorescence method, and their visual classification was carried out. It has been established that the energy of secondary characteristic x-ray radiation (CXR) for boron and iron contained in the feedstock is 3.1 and 6.3 keV, respectively. A relationship was found between the intensity of CXR pulses and the concentration of iron and boron impurities. The features of the distribution of these elements between metallurgical phases (silicon metal, slag and gas phase) when used in the smelting process with and without borate flux (colemanite) have been established. Under industrial conditions, it has been established that the transfer coefficient of boron into silicon metal is reduced when using borate flux from 76.3% to 58.36%. The transfer of iron into silicon metal from the charge remains at the same level with a slight downward trend from 93.18% to 92.12%. This may be explained by a reduction in the contact time of the molten slag accumulating on the bottom with liquid silicon metal. There is also a reduction in the consumption of charge materials when using colemanite from 6.07 to 5.635 t/t of silicon metal due to the reduction in the time of cleaning the smelting bath from viscous slag accumulated on the bottom.

Keywords Silicon metal · Smelting · Balance Fe · B · Quartz · Characteristic X—ray · Borate flux · Colemanite · Ulexite

1 Introduction

The addition of borate ore as a flux in silicon metal smelting can help reduce the problem of viscous oxide silicate melt in the SAF melt tapping process in industry. This is due to the ability of boron oxide to depolymerize the structural units of the silicate network. This effect has been previously studied using Raman spectroscopy of the processes of structural modification of the corresponding oxide melts [1]. However, on the other hand, boron, along with iron, is a harmful impurity that reduces the quality of the finished product—metal silicon and solar grade silicon. There are many studies that are exploring the possibility of removing boron and iron from silicon metal [2, 3]. In this regard, doubt may arise about the advisability of using borate ore in the smelting of silicon metal. There is a danger of boron transferring from borate ore to silicon metal. The distribution coefficient of boron between silicon metal and slag was studied under reducing conditions [4]. The results show the fundamental possibility of blocking boron reduction during the smelting process. However, these data were obtained only in laboratory conditions and the possibility of blocking boron reduction must be tested in industrial conditions. In any case, it is necessary to study the characteristics of impurities in raw materials and proposed fluxes for smelting silicon metal in order to assess the possibility of blocking boron reduction and reducing the share of iron by various methods. These works were carried out by different researchers, but so far these methods are difficult to apply on an industrial scale [5–9].

✉ Nikolay Nikolayevich Zobnin
zobninnn@mail.ru

[1] Karaganda Industrial University, Temirtau, Kazakhstan

[2] Irkutsk National Research Technical University, Irkutsk, Russia

Published online: 16 February 2024

2 Material and Method

To study the X-ray radiometric properties of quartz, the following equipment was used. X-Ray diffraction, analyzes were performed on a Philips powder diffractometer employing CuKα radiation (40 kV, 30 mA) in the range 2θ) = 10-70o at a goniometer rate of 2θ = 2o/min. For analyzed for SiO_2 and Fe_2O_3 content using XRF (X-ray Fluorescence) spectrometry ARL PERFORM'X.

To estimate the energy and intensity of secondary radiation pulses CXR – Characteristic X – ray, a system with a sensitive measuring system with semiconductor detectors of reflected X-ray radiation was used. The signal flow diagram and the operating principle of this equipment are shown in Fig. 1.

Boron-containing materials for research are presented by Ab Etiprjducts OU (Finland). X-ray phase analysis of boron-containing materials and slags was carried out on a DRON-2.0 diffractometer. Identification of diffraction maxima was carried out using the ICPDS data bank. The results of chemical analysis of boron-containing materials are presented in Table 1.

Industrial experiments were carried out in the conditions of "Tau-Ken Temir" LLP using technological equipment and the method we described earlier [10]. In the basic version, silicon metal was smelted without using borate flux, and in the experimental version, using flux.

3 Results and Discussion

To study X-ray radiometric properties, quartz from the Aktas deposit (Kazakhstan) was used. Currently, the quartz mining process does not ensure the exclusion of impurity rock. In the process of visual study of quartz, 5 groups of contaminants (impurity rocks) were identified: “black” quartz (Fig. 2), “ferruginous” quartz (Fig. 3), granite (Figs. 4 and 5), “ruby” quartz – Fig. 6, “burgundy” quartz – Fig. 7. The main mass of quartz is shown in Fig. 5. The chemical composition of all rocks is given in Table 2.

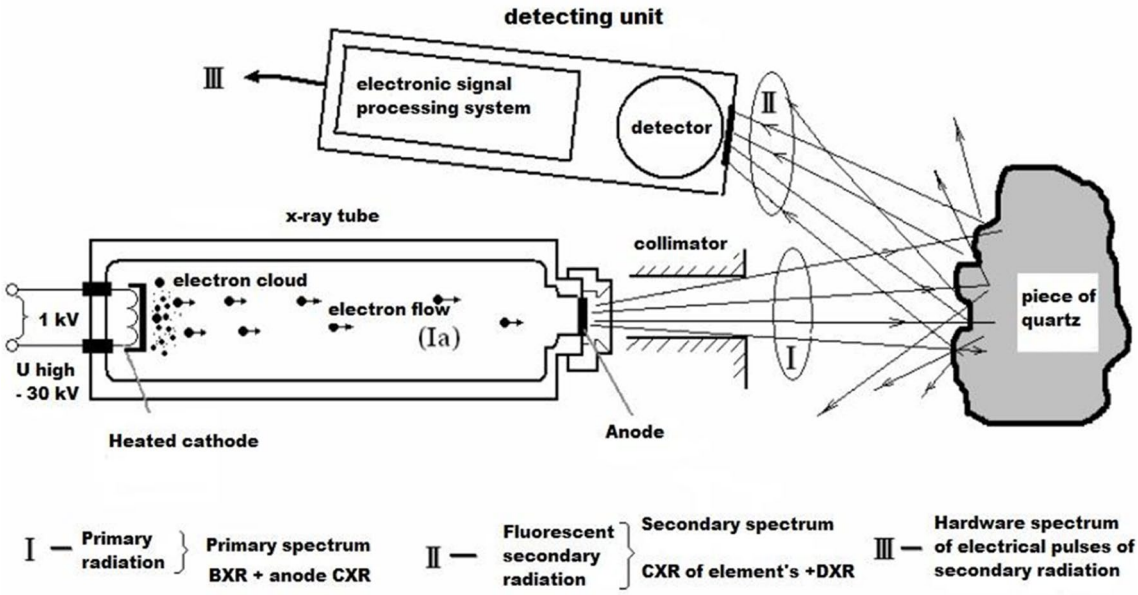

Fig. 1 Schematic diagram of the movement of signals when studying X-ray radiometric properties, BXR – Brake X—ray, CXR – Characteristic X—ray, DXR – Diffuse X—ray

Table 1 Chemical composition of boron-containing materials

Material	Content, %							Crystallization start temperature, ° C
	B_2O_3	CaO	MgO	SiO_2	Al_2O_3	Na_2O	moisture	
Colemanite	38.78	27.9	3.6 0	5.63	0.69	-	23.4 0	1004
Ulexit	35.98	18.9	4.95	4.95	0.23	5.52	29.47	940

Fig. 2 "Black" quartz

Fig. 3 Ferrous quartz

Fig. 4 Granite

Fig. 5 Bulk quartz

Fig. 6 "Ruby" quartz

Fig. 7 "Burgundy" quartz

Figure 8 shows the dependence of the number of pulses of reflected X-ray radiation over the measurement period on its energy, keV.

As can be seen from the graph, the energy of secondary characteristic x-ray radiation (CHR) for boron and iron contained in the feedstock is 3.1 and 6.3 keV, respectively.

There is a good correlation between the magnitude of the peak in the energy region of the characteristic X-ray radiation of iron and boron and the concentration of these elements in quartz, which can later be used to separate harmful impurities from raw materials using the X-ray radiometric separation method. The dependences of the intensity of pulses of characteristic secondary X-ray radiation of quartz samples on the concentration of iron and boron are presented in Figs. 9 and 10.

It should also be noted that there is a correlation between the content of iron and boron in the samples (Fig. 11), which indicates some material relationship and the possibility of the presence of complex compounds involving these elements in the samples both at the level of exogenous inclusions and at the level of incorporation into crystal structures. The results of X-ray phase analysis of boron-containing materials are presented in Fig. 12. Only the main minerals were identified in boron-containing materials: ulexite and colemanite.

Table 2 Chemical composition of quartz varieties

Name	Chemical composition, %					
	Fe_2O_3	Al_2O_3	CaO	TiO_2	B_2O_3	SiO_2
Bulk quartz	0.02	0.14	0.003	0.003	0.0006	99.8334
Granite	0.62	5.46	0.108	0.026	0.0118	93.7742
Ferrous quartz	1.23	0.16	0.011	0.005	0.0385	98.5555
"Black" quartz	5.92	3.83	0.129	0.146	0.1152	89.8598
"Ruby"	0.28	0.08	0.003	0.004	0.0023	99.6307
"Burgundy"	24.01	0.19	0.028	0.017	0.2355	75.5195

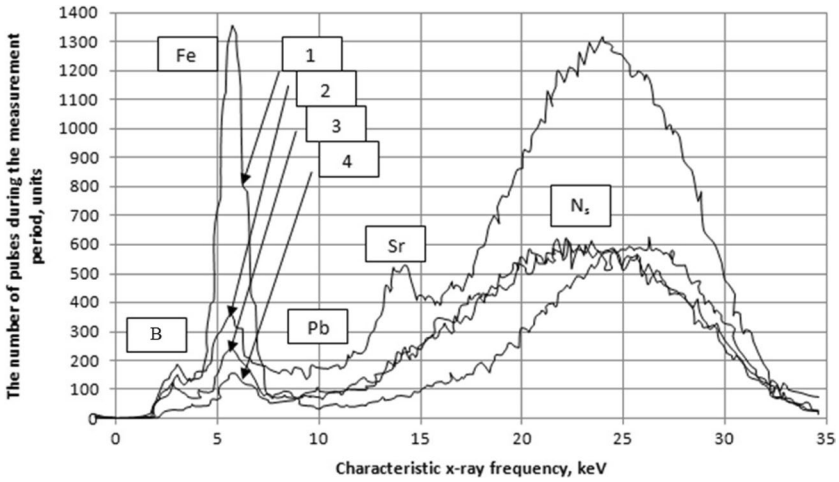

Fig. 8 Dependence of the number of pulses of reflected X-ray radiation during the measurement period on the radiation energy, keV (1 – "Black" quartz, 2 – "Ferrous" quartz, 3 – Granite, 4 – "Ruby" quartz), where N_S – secondary scattered X-ray radiation recorded from a piece of raw material together with the characteristic radiation of the elements

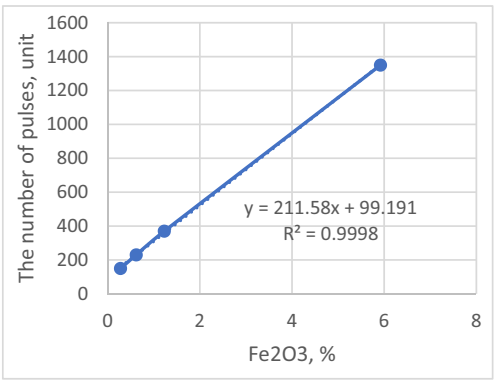

Fig. 9 Dependence of CXR intensity (Fe) on %, Fe_2O_3 in a quartz sample

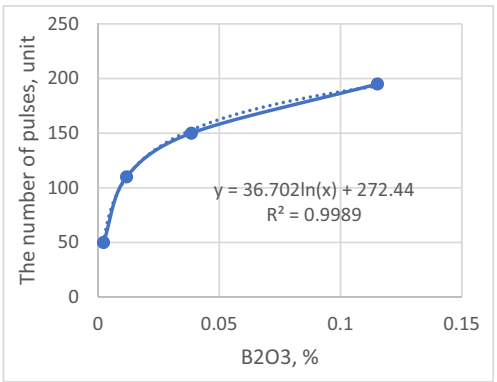

Fig. 10 Dependence of CXR intensity (B) on %, B_2O_3 in a quartz sample

The basic period of industrial research was characterized by the presence of slag-forming impurities in the composition of raw materials. This led to the formation of small amounts (3–6%) of molten slag in the furnace bath. For operational stability, every effort was made to ensure that these slags were completely removed during melt tapping. Slag (55–60 kg per 1 ton of silicon) is high-silicon with a fairly high melting point and viscosity. The actual density of the slag is 2.5–2.8 kg/m^3 which is higher than or remains at the silicon level 2.4–2.6 kg/m^3. That is, the slag melt is somewhat heavier than the silicon melt, so it gradually accumulates under a layer of liquid silicon. Chemical composition of slag is: SiO_2 – 75–80%; Al_2O_3 – 5–7%; CaO – 11–15%. The melting point of slag is about 1500 °C. The silicon carbide content in the slag can reach 10–30%, which significantly increases the melting point (more than 1600 °C) and viscosity. The accumulation of refractory and viscous slag at the bottom of the furnace bath contributes to the transition of the reaction zone to the middle horizons of the bath, which, in fact, is observed in reality.

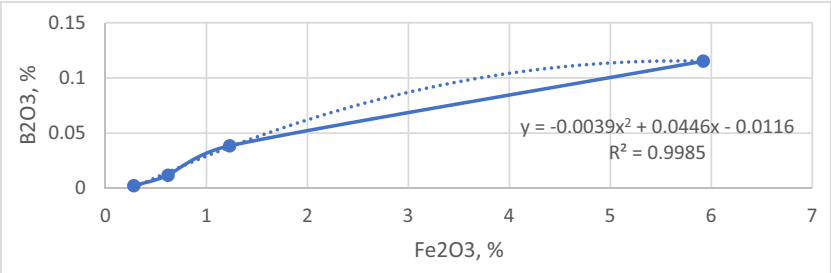

Fig. 11 Relationship between %, Fe_2O_3 and B_2O_3 in a quartz sample

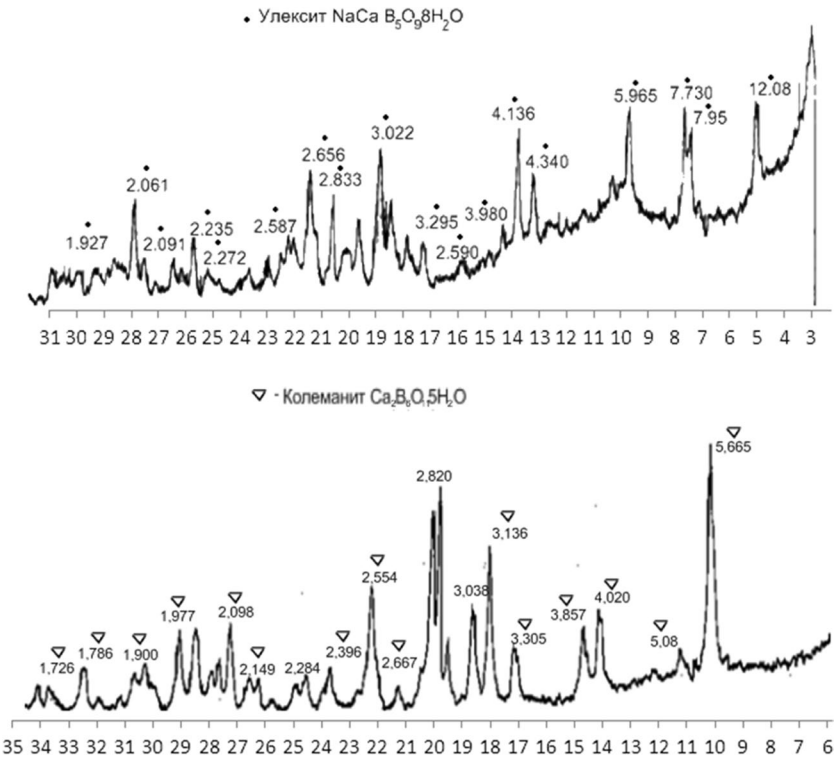

Fig. 12 X-ray diffraction patterns of initial boron-containing materials

Due to its low density, molten silicon is located on top of the slag. Therefore, low activity of the discharged silicon is observed at the tapping, which rather seeps through the slag melt. In the base period, without the addition of boron-containing fluxes, periodic cleaning operation of the furnace was carried out to remove the slag accumulated on the bottom. At the same time, the supply of charge into the bath was limited or completely stopped. The crucibles were opened, the reducing silicon was sublimated. In this case, it became possible to warm up the molten slag, which is periodically drained. During melting, the yield of silicon decreases or completely stops due to its sublimation into the gas phase. Without this, melting is impossible, since there will be silicon on the surface of the slag, which will not allow the slag to be heated. Therefore, this silicon has to be overheated above normal. This led to its secondary oxidation by air through open gas cavities, followed by sublimation in the form of silicon monoxide. The duration of melting in cases of severe slagging of the hearth reached 24 h to sufficiently completely clean the furnace bath from slag.

During cleaning operation, the current load was reduced and the voltage on the bath was increased. The disadvantage of this method is the increase in the temperature of the process gases removed into gas cleaning system, as well as the increased thermal load on the elements of the short network. To reduce the penetration (melting) time or completely eliminate the need for this technological operation, an experimental period was carried out in the furnace using boron-containing flux (colemanite) to clean the bath. Visual observation of the smelting process showed that the use of colemanite in the smelting of silicon metal has a positive effect, namely, expansion of the furnace bath is observed, tapping proceeds without difficulty. The addition of colemanite proved to be a low-melting mixture and the furnace bath was in normal condition.

Tables 3 and 4 present the balance of iron and boron during the base and experimental periods of furnace operation, respectively. The duration of each period was 3 months. As can be seen from a comparison of the balances of the base and experimental periods, the addition of colemanite in small quantities, about 2 kg/t of silicon metal, ensured a reduction in the consumption of charge materials per ton of finished product.

So, if in the base period the production of 1 ton of silicon metal required 6.07 tons of charge, then with the addition of colemanite the consumption was reduced to 5.635 tons. This can be explained by the fact that in the base period about 10 cleaning operations were carried out in order to clean the smelting bath from accumulated slag. During these operations, strong evaporation of silicon in the form of monoxide and burning of carbonaceous materials occurred. In this case, there was no accumulation of silicon metal, because all useful components passed into the gas phase and left the furnace in the form of dust (silica fume). This is confirmed by the fact that in the base period the amount of silica fume was significantly greater than in the experimental period—1.2138 t/t and 1.0052 t/t of silicon metal, respectively. During the experimental period, melting operations were completely excluded. At moments when, according to

Table 3 Material balance of iron and boron in the base period of silicon metal smelting

RAW MATERIAL							
Material	Expenditure rate, t / t	B, %	Go B into		Fe,%	Go Fe into	
			kg	%		kg	%
Quartz	3.20	0.0006	0.0192	1.81	0.120	3,840	63.63
Charcoal	0.64	0.0722	0.4620	43.50	0.041	0.256	4.24
Coal	0.93	0.0158	0.1469	13.83	0.122	1.116	18.49
Semi coke	0.35	0.0298	0.1043	9.82	0.221	0.770	12.76
Graphite electrode	0.11	0.1523	0.1675	15.77	0.010	0.011	0.18
Wood chips	0.84	0.0193	0.1621	15.26	0.005	0.042	0.70
Total	6.07		1.0621			6.035	
FINISHED PRODUCTS							
Material	Expenditure rate, t / t	B, %	Go B out		Fe,%	Go Fe out	
			kg	%		kg	%
Silicon metal	1.0000	0.0810	0.8104	76.3	0.5622	5.622	93.18
Slag	0.0885	0.2376	0.2102	19.8	0.2727	0.241	4.00
Silica fume	1.2138	0.0033	0.0410	3.9	0.014 0	0.170	2.82
Total	2.3023		1.0617			6.033	

Table 4 Material balance of iron and boron in the experimental period of silicon metal smelting

RAW MATERIAL							
Material	Expenditure rate, t / t	B, %	Go B into		Fe,%	Go Fe into	
			kg	%		kg	%
Quartz	3,051	0.0007	0.0214	1.73	0.10	3.0510	60.63
Charcoal	0.595	0.0699	0.4159	33.66	0.03	0.1785	3.55
Coal	0.88	0.0163	0.1434	11.61	0.14	1.2320	24.48
Semi coke	0.248	0.0311	0.0771	6.24	0.21	0.5208	10.35
Graphite electrode	0.088	0.1877	0.1652	13.37	0.02	0.0176	0.35
Wood chips	0.771	0.0223	0.1719	13.91	0.002	0.0154	0.31
Colemanite	0.002	12,035	0.2407	19.48	0.86	0.0172	0.34
Total	5.635		1.2356			5.0325	
FINISHED PRODUCTS							
Material	Expenditure rate, t / t	B, %	Go B out		Fe,%	Go Fe out	
			kg	%		kg	%
Silicon metal	1.0000	0.0721	0.7210	58.36	0.464	4.640	92.12
Slag	0.0922	0.5228	0.4820	39.02	0.267	0.246	4.89
Silica fume	1.0052	0.00322	0.0324	2.62	0.015	0.151	2.99
Total	2.0974		1.2354			5.037	

external signs, a critical amount of slag had accumulated in the furnace, after the last tapping, the gas cavities near the electrodes were opened and 50 to 200 kg of colemanite were given under the electrodes. The amount of colemanite was determined depending on the degree of slagging of the smelting bath. The more signs, such as difficulties in tapping, low temperature of silicon metal, etc., the greater the amount of colemanite is.

Despite the fact that colemanite contains much more boron than other components of the charge, the income of elemental boron per ton of finished product increased slightly—1.062 kg/t and 1.235 kg/t for the base and experimental periods, respectively. This became possible due to the fact that the consumption of colemanite is very small. A small increase in boron income was also ensured by the fact that the consumption of other charge materials (charcoal, wood chips, etc.), which are also sources of boron, was reduced.

It should be especially noted that the addition of colemanite ensured a reduction in the degree of transfer of boron into silicon metal from 76.3% to 58.36% in the base and experimental periods, respectively. At the same time, the distribution coefficient of boron, $L_B = W_{(B)}/W_{[B]}$ was 0.259 for the base period and 0.668 for the experimental period. These data are consistent with the data presented in the literature [4]. It should be noted that the authors have achieved significantly better results in this regard. So initially they received the distribution coefficient of boron at the level of 0.206 at an exposure of 0.6 h using master slag with the composition: SiO_2 – 63.2%; CaO – 36.3%. After 3 h of exposure of the silicon metal over the master slag, L_B increased to 1,649 and to 2,138 at an exposure of 9 h [4]. However, in the conditions of industrial production, it is not possible to provide such a long exposure time. The realistic value is 0.50–0.75 h. In addition, in industrial conditions, to increase the content of CaO in the slag to 35–40%, it is necessary to significantly increase the consumption of lime in the charge. This can lead to contamination of the silicon metal with calcium and further the need to increase the purge time during the oxidative refining process. An increase in the purge time usually leads to an increased loss of silicon as a result of oxidation.

Under our conditions, the concentration of boron in silicon metal decreased slightly from 0.081% to 0.0721% in the baseline and experimental periods, respectively. The result obtained seems at first glance to be contradictory. We expected that with the addition of colemanite, the concentration of boron in silicon metal would be increased. In reality, it turned out the other way around. Logically, this finding can be explained by the fact that in the base period the slag accumulated in the furnace and was in contact with liquid silicon metals for a long time. In this case, the silicon metal was saturated with impurities, including boron. When colemanite was added, the slag did not accumulate, quickly left the furnace, and the contact time of the slag with the silicon metal was significantly reduced. Due to this, the transfer of impurities from slag to silicon metal was limited. This is indirectly confirmed by an increase in the boron concentration in the slag from 0.2376% to 0.5228% in the base and experimental periods, respectively.

The distribution of iron practically did not change when colemanite was added into the charge. One can note a slight increase in the transition of iron to slag from 4.0% to 4.89%. Perhaps this is also due to the reduction in the contact time of liquid molten slag and silicon metal on the bottom of the furnace.

The experiments were carried out only with the use of colemanite due to organizational possibilities. Whenever possible, experiments will also be carried out using ulexite as a boron-containing flux.

4 Conclusions

A visual classification of impurity rocks in the composition of quartz was carried out. The radiographic features of charge materials for the production of silicon metal have been determined. It has been established that the energy of secondary characteristic x-ray radiation (CXR) for boron and iron contained in the feedstock is 3.1 and 6.3 keV, respectively. A correlation has been established between the intensity of CXR pulses and the concentration of iron and boron impurities. Under industrial conditions, the possibilities of the transfer of impurity elements into silicon metal have been established when borate flux (colemanite) is used in the smelting process and without it. It was found that the transfer coefficient of boron into silicon metal is reduced when using colemanite from 76.3% to 58.36%. The transfer of iron into silicon metal from the charge remains at the same level with a slight downward trend from 93.18% to 92.12%. This can probably be explained by a decrease in the contact time of the molten slag accumulating on the bottom with liquid silicon metal. The addition of boron-containing flux (colemanite) reduces the consumption of charge materials from 6.07 to 5.635 t/t of metal silicon by reducing the time required to clean the melting bath from viscous slag accumulated on the bottom. The concentration of boron and iron impurities in silicon metal is reduced. The furnace is operating normally. There are no difficulties during tapping, the amount of dust and gas emissions is reduced.

Author Contributions All four authors contributed significantly to the conception, design, and execution of the study, as well as the analysis and interpretation of the data. Each author has been actively involved in

drafting and critically revising the manuscript for important intellectual content. The specific contributions of each author are outlined below:

Alexandr Ilin: Contributed to the design of the study, conducted experiments, and played a key role in funding acquisition. Participated in drafting and revising the manuscript.

Nikolay Zobnin: Contributed to the study's conception, design, and coordination. Participated in data interpretation and manuscript revision. Provided valuable intellectual input throughout the research process.

Irina Pikalova: Provided substantial contributions to the acquisition of data, data analysis, and interpretation. Played an active role in drafting and critically revising the manuscript for important intellectual content.

Nina Nemchinova: Participated in the design and coordination of the study, contributed to data analysis, and played a crucial role in manuscript preparation and revision.

All authors have read and approved the final version of the manuscript and agree to be accountable for all aspects of the work, ensuring that questions related to the accuracy or integrity of any part of the work are appropriately investigated and resolved.

This collaborative effort reflects a balanced and comprehensive contribution from each author, resulting in a cohesive and well-rounded research study.

Funding The research was funded by the Science Committee of the Ministry of Education and Science of the Republic of Kazakhstan (Grant No. AP19177929).

Data Availability All data reported in this research can be obtained from the corresponding author upon request.

Declarations

Ethics Approval The authors confirm that this work was written in compliance with the principles of scientific ethics, the use of correct borrowings.

Consent to Participate The authors of the article confirm their consent to participate in this research.

Consent for Publication The authors of the article confirm their agreement to be acknowledged as the authors of the paper.

Competing Interests The authors declare no competing interests.

References

1. Kline Jeff, Tangstad Merete, Tranell Gabriella (2014) A Raman spectroscopic study of the structural modifications associated with the addition of calcium oxide and boron oxide to silica. Miner, Met Mater Soc ASM Int 46:62–73. https://doi.org/10.1007/s11663-014-0194-9
2. Chenghao Lu, Tang T, Sheng Z, Xing P, Luo X (2017) Improved removal of boron from metallurgical-grade Si by $CaO-SiO_2-CaCl_2$ slag refining with intermittent $CaCl_2$ addition. Vacuum 143:7–13
3. Ding Z, Ma W, Wei K, Jijun Wu, Zhou Y, Xie K (2012) Boron removal from metallurgical-grade silicon using lithium containing slag. J Non-Cryst Solids 358:2708–2712
4. Jakobsson LK, Tangstad M (2014) Distribution of Boron Between Silicon and $CaO-MgO-Al_2O_3-SiO_2$ Slags. Metall Mater Trans B. 45B:1644–1655
5. Ben FM, Gallala W, Abdeljaouad S (2016) Quartz sand beneficiation using magnetic and electrostatic separation to glass industries. J New Technol Mater JNTM 06(01):60–72
6. Deniz AF, Abakay TH, Bozkurt V (2011) Removal of Impurities from Tailing (Quartz) Obtained from Bitlis Kyanite Ore by Flotation Method. Int J Appl Sci Technol 1(1):74–81
7. Hacifazlioglu H (2014) Enrichment of silica sand ore by cyclojet flotation cell. Sep Sci Technol 49:1623–1632
8. Soufiane B, Mohamed B, Abde SC (2015) Removal of iron from sandstone by magnetic separation and leaching: case of El- aouana deposit (Algeria). Min Sci 22:33–44
9. Tuncuk A, Akcil A (2014) Removal of iron from quartz ore using different acids a laboratory-scale reactor study. Mineral Processing & Extractive Metall Rev 35(4):217–228
10. Zobnin NN, Torgovets AK, Pikalova IA, Yussupova YS, Atakishiyev SA (2018) Influence of thermal stability of quartz and the particle size distribution of burden materials on the process of smelting of electro thermal metallurgical silicon. Orient J Chem 34(2):1120–1125. https://doi.org/10.13005/ojc/340265